



Zeroing neural network with comprehensive performance and its applications to time-varying Lyapunov equation and perturbed robotic tracking

Zeshan Hu^a, Kenli Li^{a,*}, Keqin Li^{a,b}, Jichun Li^c, Lin Xiao^{d,*}

^a College of Information Science and Electronic Engineering, Hunan University, Changsha 410082, China

^b Department of Computer Science, State University of New York, New Paltz, NY12561, USA

^c School of Computer Science and Electronic Engineering, University of Essex, Colchester CO4 3SQ, UK

^d Hunan Provincial Key Laboratory of Intelligent Computing and Language Information Processing, Hunan Normal University, Changsha 410081, China

ARTICLE INFO

Article history:

Received 26 November 2019

Revised 21 June 2020

Accepted 4 August 2020

Available online 1 September 2020

Communicated by Long Cheng

Keywords:

Finite-time convergence

Noise tolerance

Stable residual error

Tracking control

Zeroing Neural Network (ZNN)

ABSTRACT

The time-varying Lyapunov equation is an important problem that has been extensively employed in the engineering field and the Zeroing Neural Network (ZNN) is a powerful tool for solving such problem. However, unpredictable noises can potentially harm ZNN's accuracy in practical situations. Thus, the comprehensive performance of the ZNN model requires both fast convergence rate and strong robustness, which are not easy to accomplish. In this paper, based on a new neural dynamic, a novel Noise-Tolerance Finite-time convergent ZNN (NTFZNN) model for solving the time-varying Lyapunov equations has been proposed. The NTFZNN model simultaneously converges in finite time and have stable residual error even under unbounded time-varying noises. Furthermore, the Simplified Finite-time convergent Activation Function (SFAF) with simpler structure is used in the NTFZNN model to reduce model complexity while retaining finite convergence time. Theoretical proofs and numerical simulations are provided in this paper to substantiate the NTFZNN model's convergence and robustness performances, which are better than performances of the ordinary ZNN model and the Noise-Tolerance ZNN (NTZNN) model. Finally, simulation experiment of using the NTFZNN model to control a wheeled robot manipulator under perturbation validates the superior applicability of the NTFZNN model.

© 2020 Elsevier B.V. All rights reserved.

1. Introduction

The Lyapunov equation plays a crucial part in many scientific and engineering fields. For instance, it can be applied in communication [1], control theory [2,3] and automatic control [4,5]. Furthermore, Lyapunov equation is indispensable in the domain of optimal control. Thus, the solution of Lyapunov equation has earned a large amount of efforts on account of its extensive applications. For solving Lyapunov equation, approaches that have the longest history should be traditional numerical algorithms. In [6], an iterative algorithm was proposed to tackle Lyapunov equation with Markov jump. Other types of numerical algorithms for Lyapunov equation have also been investigated. [7] proposed an iterative algorithm based on the gradient to solve this problem, while [8] presented a method based on minimal residual error. However, the minimum time complexity of these numerical algorithms is

about the cube of dimensions of input matrix. Thus, solving large scale Lyapunov equations using these numerical algorithms becomes a time consuming task. The large time cost of numerical algorithms has considerably limited their application ranges, especially for online Lyapunov equation problem.

Nowadays, we can accelerate many algorithms by taking advantage of hardware or software level parallelism, but this approach is hard for above mentioned numerical algorithms because of their serial processing nature. Therefore, Artificial Neural Networks (ANNs) including the Recurrent Neural Networks (RNNs) as other types of approaches, have been found efficient in solving various numerical computation, optimization and robot control problems [9–13] due to their parallel and distributed computing properties. Gradient-based Neural Network (GNN) is a variation of RNN and was investigated for the online stationary Lyapunov equation [14–17]. GNN uses the norm of error matrix as its performance index and the neural network will evolve along the gradient-descent direction until its performance index converges to zero. GNN performs well in stationary Lyapunov equation problems,

* Corresponding author.

E-mail addresses: lik@hnu.edu.cn (K. Li), xiaolin860728@163.com (L. Xiao).

but it suffers from large residual error on solving time-varying Lyapunov equations and such error exists even after infinite time of evolving, which promotes researchers to overcome this drawback by discovering new neural network models.

Under such background, Zeroing Neural Network (ZNN) as a special type of RNN was proposed and utilized in Refs. [18–21]. This kind of RNN model utilizes the velocity information of time-varying coefficients and uses the error matrix instead of its norm as performance index, successfully surpassing GNN model on solving both stationary and nonstationary Lyapunov equations. Nevertheless, the ordinary ZNN model is far from being perfect because it uses linear function as activation function and can only converge to the solution exponentially. That is, its error cannot converge to zero in finite time. Recently, many research works about speeding up the convergence speed of ANNs are springing up [22–24]. Therefore, to improve the convergence speed of the ordinary ZNN model, a finite-time convergent ZNN model which exploited the Sign-Bi-Power (SBP) activation function is presented in Ref. [25]. Another practical problem is that ZNN usually works in an environment that exists various noise and this can potentially decrease the accuracy of the neural network, but the general ZNN design formula didn't take this factor into account. Thus, [26–28] designed a Noise-Tolerance ZNN (NTZNN) model to enhance ZNN model's robustness against additive noise. However, NTZNN's activation function is linear function and cannot be changed, so that it cannot converge in finite time. In this paper, we present a Noise-Tolerance Finite-time convergent ZNN (NTFZNN) model for the time-varying Lyapunov equation problem following the motivation that both finite-time convergence and noise suppression ability are highly demanded in ZNN applications [29]. The NTFZNN model not only converges to the accurate solution of time-varying Lyapunov equation in finite time in noise-free environments, but also have less stable residual error than the NTZNN model within additive noise polluted environment.

The main contributions of this paper are summarized as below:

- 1) A novel NTFZNN model is developed for solving time-varying Lyapunov equation problem, which possesses finite-time convergence and powerful additive noise suppression ability at the same time.
- 2) Using the SFAF (Simplified Finite-time convergent Activation Function), the NTFZNN_{SFAF} (NTFZNN using SFAF) model is proposed, which has simpler structure and lower calculation complexity than the NTFZNN_{SBP} (NTFZNN using SBP) model but still being finite-time convergent.
- 3) The convergence time upper bound and stable residual error upper bound of the NTFZNN model have both been quantitatively analyzed and then validated by simulation experiments. Besides, in the robustness analysis, the more practical time-varying unknown noises are investigated rather than the usual constant or limited known noises.

The rest of this paper is organized into 6 sections. In Section 2, the problem description and some preliminaries of the time-varying Lyapunov equation are provided for the following discussion and analyses. In Section 3, the NTFZNN model is designed for solving the time-varying Lyapunov equation, and two finite-time convergent activation functions have been introduced. In Section 4, the NTFZNN model's convergence performance in noise-free environment and robustness performance when perturbed by additive noises have been analyzed in detail. In Section 5, numerical simulations and comparisons are presented to verify the previous theoretical conclusions. In Section 6, the NTFZNN model is successfully applied in controlling a mobile robot manipulator to track the desired path with additive noise perturbation, which

has further validated the NTFZNN model's applicability and superiority. Section 7 concludes this paper briefly.

2. Problem description and preliminaries

In this paper, the problem we mainly concerned about is solving the time-varying Lyapunov equation. Let $M(t) \in \mathbb{R}^{n \times n}$ be a nonstationary coefficient matrix with $Q(t) \in \mathbb{R}^{n \times n}$ being a nonstationary symmetric positive-definite matrix. We have following equation:

$$M^T(t)\dot{X}(t) + X(t)M(t) = -Q(t). \quad (1)$$

Then, the above equation is widely known as the Lyapunov equation, where $X(t) \in \mathbb{R}^{n \times n}$ is a unique time-varying matrix that we should obtain given that $M(t)$ and $Q(t)$ both satisfied the unique solution condition [17]. In the following paper, we use $A(t) \in \mathbb{R}^{n \times n}$ to denote the precise solution of (1) for efficient expression. Under such preliminaries, in this paper, we focus on proposing a NTFZNN (Noise-Tolerance Finite-time convergent ZNN), which not only makes use of the latest activation function, but also newly proposed novel activation function.

Generally speaking, in the field of solving time-varying problems, zeroing neural network is a more powerful tool when compared with conventional gradient-based neural network, because it eliminates lagging errors which exist in the latter one. Furthermore, [30] shows that ordinary ZNN model can deal with time-varying Lyapunov equation efficiently as well as converge to accurate solution exponentially. To lay the foundation of this paper, the design process of ordinary ZNN model for this problem (1) can be separated into following procedures:

- 1) Firstly, construct a matrix type error function to evaluate the difference between state solution of neural network and theoretical solution of (1):

$$E(t) = M^T(t)\dot{X}(t) + X(t)M(t) + Q(t) \in \mathbb{R}^{n \times n}. \quad (2)$$

- 2) Then, as the unique solution of (1), $A(t)$ is clearly the zero point of above error function. For the purpose of forcing $E(t)$ to converge to zero, the ZNN model uses the following evolution formula:

$$dE(t)/dt = -\mu \mathcal{A}(E(t)), \quad (3)$$

where μ is a design parameter satisfying $\mu > 0$, $\mathcal{A}(\cdot) : \mathbb{R}^{n \times n} \rightarrow \mathbb{R}^{n \times n}$ denotes a mapping matrix with each of its element being the same activation function.

- 3) Finally, substituting (2) into (3) leads to the following ordinary ZNN model for the time-varying Lyapunov equation problem:

$$M^T(t)\dot{X}(t) + \dot{X}(t)M(t) = -\dot{M}^T(t)X(t) - X(t)\dot{M}(t) - \dot{Q}(t) - \mu \mathcal{A}(M^T(t)X(t) + X(t)M(t) + Q(t)), \quad (4)$$

where state solution $X(t)$ will change smoothly along with the evolution of ZNN model as time goes on. Starting from initial value $X(0) \in \mathbb{R}^{n \times n}$, $X(t)$ converges to the accurate solution $A(t)$ asymptotically. Note that, if linear activation function $f(x) = x$ is used, model (4) possesses exponential convergence property [30].

The ordinary ZNN model (4) is enough for theoretical analysis. But if we want to do simulation experiments or implement this model, the ordinary ZNN model (4) can be transformed into following explicit ordinary ZNN model:

$$N_1(t)\dot{\mathbf{x}}(t) = -\dot{N}_1(t)\mathbf{x}(t) - \dot{N}_2(t) - \mu \mathcal{A}(N_1(t)\mathbf{x}(t) + N_2(t)), \quad (5)$$

where we define the operation $A \oplus B = A \otimes I + I \otimes B$ with I being identity matrix. Under such definition, other parameters in (5) are: $N_1(t) = M^T(t) \oplus M^T(t) \in \mathbb{R}^{n^2 \times n^2}$, $N_2(t) = \text{vec}(Q(t)) \in \mathbb{R}^{n^2}$ and $\mathbf{x}(t) = \text{vec}(X(t)) \in \mathbb{R}^{n^2}$. Besides, the symbol \otimes stands for the well known Kronecker product, whose detail information can be found in [17,31]. Another symbol $\text{vec}(\cdot)$ denotes the operation that stacks all column vectors of its input matrix into a single column vector. Mapping matrix in (5) is resized to $\mathcal{A}(\cdot) : \mathbb{R}^{n^2} \rightarrow \mathbb{R}^{n^2}$ due to vectorization.

3. Design of noise-tolerance finite-time convergent Zeroing Neural Network

The ordinary ZNN model introduced in Section 2 is able to handle the nonstationary Lyapunov equation well in the ideal noise-free environment. However, because continuous ZNN models are mainly implemented in analog circuits, there are many factors that may create noises. These factors include round-off error, circuit implementation errors and so on, which can result in the great loss for ZNN model (4) in accuracy. Therefore, we propose a novel NTFZNN model with better noise suppression ability for time-varying Lyapunov equation. To monitor the computation process of the problem, NTFZNN uses the same error matrix as in the ordinary ZNN model:

$$E(t) = M^T(t)X(t) + X(t)M(t) + Q(t) \in \mathbb{R}^{n \times n}. \quad (6)$$

Then, the design formula of NTFZNN becomes different from the ordinary ZNN model (4), since it introduces an integral item into the formula to enhance its noise tolerant ability. The NTFZNN model's design formula is presented as below:

$$\dot{E}(t) = -\mu \mathcal{A}_1(E(t)) - \xi \mathcal{A}_2 \left(E(t) + \mu \int_0^t \mathcal{A}_1(E(\tau)) d\tau \right), \quad (7)$$

where $\mathcal{A}_1(\cdot) : \mathbb{R}^{n \times n} \rightarrow \mathbb{R}^{n \times n}$ and $\mathcal{A}_2(\cdot) : \mathbb{R}^{n \times n} \rightarrow \mathbb{R}^{n \times n}$ represent monotone increasing mapping arrays which consist of the same activation functions respectively. Theoretically speaking, $\mathcal{A}_1(\cdot)$ and $\mathcal{A}_2(\cdot)$ can be chosen arbitrarily as long as they satisfy the requirement of being finite-time convergent. In this paper, we set them to be the same to facilitate the following further analyses. Besides, $\mu > 0$ and $\xi > 0$ are design parameters used to adjust the neural network's convergence speed and noise suppression ability. Now, the NTFZNN model (7) can be expanded by substituting (6) into (7), and then we get

$$\begin{aligned} M^T(t)\dot{X}(t) + \dot{X}(t)M(t) = & -\dot{M}^T(t)X(t) - X(t)\dot{M}(t) \\ & -\dot{Q}(t) - \mu \mathcal{A}_1(E(t)) - \xi \mathcal{A}_2 \\ & \left(E(t) + \mu \int_0^t \mathcal{A}_1(E(\tau)) d\tau \right). \end{aligned}$$

The above neural dynamic is equivalent to the NTFZNN model (7) and can also be transformed into explicit NTFZNN model similar to (5):

$$\begin{aligned} N_1(t)\dot{\mathbf{x}}(t) = & -\dot{N}_1(t)\mathbf{x}(t) - \dot{N}_2(t) - \mu \mathcal{A}_1(N_1(t)\mathbf{x}(t) + N_2(t)) \\ & - \xi \mathcal{A}_2(N_1(t)\mathbf{x}(t) + N_2(t)) \\ & + \mu \int_0^t \mathcal{A}_1(N_1(\tau)\mathbf{x}(\tau) + N_2(\tau)) d\tau, \end{aligned} \quad (8)$$

where $N_1(t), N_2(t), \mathbf{x}(t)$ are all defined the same as in (5).

It should be pointed out that researchers have investigated the performance of the ordinary ZNN model under noise perturbed environment, some methods with the internal noise-tolerance ability have been proposed to tackle this problem [26,32]. One of these methods is called Noise-Tolerance ZNN (NTZNN) model [26], which is also the inspiration source of our NTFZNN model. The NTZNN model uses following design formula:

$$\dot{E}(t) = -\mu E(t) - \xi \int_0^t E(\tau) d\tau, \quad (9)$$

where the definition of $E(t) \in \mathbb{R}^{n \times n}$, $\mu > 0$ and $\xi > 0$ are the same as in (7). NTZNN performs well in the presence of perturbation, even if the noise is in the form of additive noise that increases linearly with time. But since the NTZNN model lacks of activation function, which is an important element contributing to convergence speed of the ZNN model, it can only achieve the exponential convergence. This motivates us to propose the NTFZNN model to realize both noise tolerant and finite-time convergent properties on solving Lyapunov equation.

In-depth researches about ZNN models have revealed that the choice of activation functions plays an important role in convergence performance of ZNN models including their variations. Furthermore, nonlinear activation functions usually speed up the convergence process of ZNN models. Particularly, some functions can even realize finite-time convergence, one of them being the well known Sign-Bi-Power (SBP) function [33], whose equation is

$$\psi_{\text{SBP}}(e_{ij}) = \frac{1}{2} \text{sgn}^p(e_{ij}) + \frac{1}{2} \text{sgn}^{\frac{1}{p}}(e_{ij}), \quad (10)$$

with $p \in (0, 1)$, and the definition of $\text{sgn}^p(e_{ij})$ is as follows:

$$\text{sgn}^p(e_{ij}) = \begin{cases} e_{ij}^p, & e_{ij} > 0, \\ 0, & e_{ij} = 0, \\ -|e_{ij}|^p, & e_{ij} < 0, \end{cases}$$

where e_{ij} is the ij th element of error matrix $E(t)$. Following the idea of SBP activation function, researchers found that the SBP function is computing intensive due to the power operation on floating point number p , which not only increases the burden of computation but also requires more complex structure. A novel Simplified Finite-time convergent Activation Function (SFAF) based on the SBP function is thus proposed [34], whose definition is

$$\psi_{\text{SFAF}}(e_{ij}) = \beta_1 \text{sgn}^p(e_{ij}) + \beta_2 e_{ij}, \quad (11)$$

where $\beta_1 > 0$ and $\beta_2 > 0$ are design parameters. It is clearly shown that SFAF has simpler structure than traditional SBP function. Besides, SFAF can accelerate the ZNN model to finite-time convergence with even lower upper bound of convergence time.

For concise expression, in the following paper, the NTFZNN model using SBP and SFAF activation functions will be named as the NTFZNN_{SBP} model and the NTFZNN_{SFAF} model respectively. Another thing should be pointed out is that our NTFZNN model only uses SBP (10) and SFAF (11) as activation functions in the following paper in order to achieve finite-time convergence.

4. Theoretical analysis of noise-tolerance finite-time convergent Zeroing Neural Network

In this section, we focus on proving NTFZNN to be globally stable, computing the convergence time upper bound, and analyzing inherent noise suppression ability of the NTFZNN model (7). All of these theoretical analyses eventually illustrate the superiority of our NTFZNN model. As it has been shown in Section 3, the NTFZNN model formula (7) is equivalent to the formula (8) and the latter one is mainly used in the following analyses and experiments. In addition, the error matrix $E(t)$ in (7) becomes the error vector $\mathbf{e}(t) = N_1(t)\mathbf{x}(t) + N_2(t)$ in (8). Therefore, the design formula of NTFZNN model (7) can be transformed into the vector form:

$$\dot{\mathbf{e}}(t) = -\mu \mathcal{A}_1(\mathbf{e}(t)) - \xi \mathcal{A}_2 \left(\mathbf{e}(t) + \mu \int_0^t \mathcal{A}_1(\mathbf{e}(\tau)) d\tau \right), \quad (12)$$

where $\mathbf{e}(t) \in \mathbb{R}^{n^2}$ is obtained by stacking all the column vectors of $E(t)$ into a single column vector. In addition, due to the vectorization

of (7), $\mathcal{A}_1(\cdot) : \mathbb{R}^{n^2} \rightarrow \mathbb{R}^{n^2}$ and $\mathcal{A}_2(\cdot) : \mathbb{R}^{n^2} \rightarrow \mathbb{R}^{n^2}$ become vector-valued mapping arrays with their elements being unchanged. In addition, applying the same technique as above, the ordinary ZNN model (3) can be transformed into the following vector-valued form:

$$\dot{\mathbf{e}}(t) = -\mu \mathcal{A}(\mathbf{e}(t)), \quad (13)$$

where $\mathcal{A}(\cdot) : \mathbb{R}^{n^2} \rightarrow \mathbb{R}^{n^2}$ becomes mapping array of vectors with the same elements. In order to lay the foundations for the ensuing theoretical analyses, we have the following lemmas.

Lemma 1 [35]. Consider a system $\dot{x} = f(x), x \in \mathbb{R}^n, f : \mathbb{R}^n \rightarrow \mathbb{R}^n$ which has a equilibrium point $x = 0$ meaning $f(0) = 0$. Besides, there exists a Lyapunov candidate function $V : \mathbb{R}^n \rightarrow \mathbb{R}$ that satisfies 1) $V(x) = 0$ if and only if $x = 0$; 2) $V(x) > 0$ if and only if $x \neq 0$; 3) $\dot{V}(x) < 0$ is true for all $x \neq 0$. Then, such system is said to be globally asymptotically stable.

Lemma 2 [36]. Given smoothly time-varying error vector $\mathbf{e}(t) \in \mathbb{R}^{n^2}$ in (13). If a monotonically-increasing odd mapping array $\mathcal{A}(\cdot)$ is used, then the ordinary ZNN dynamic (13) is globally stable and its error vector $\mathbf{e}(t)$ can converge to the equilibrium point $\mathbf{e}(t) = 0$ starting from a random initial state $\mathbf{e}(0)$.

4.1. Convergence analysis

In this section, we will prove the global asymptotic stability of NTFZNN model (7), the convergence time upper bound of NTFZNN model (7) on solving time-varying Lyapunov equation will also be computed.

Theorem 1. When solving time-varying Lyapunov Eq. (1), NTFZNN model (12) is globally stable, meaning that the state solution of NTFZNN globally converges to the accurate solution of (1).

Proof. The design formula of NTFZNN model (12) gives every element of $\mathbf{e}(t)$ the same inherent dynamics, and thus we only need to consider the i th element. This subsystem with $\forall i \in \{1, 2, 3, \dots, n^2\}$ can be written as:

$$\dot{e}_i(t) = -\mu \Psi_1(e_i(t)) - \xi \Psi_2\left(e_i(t) + \mu \int_0^t \Psi_1(e_i(\tau)) d\tau\right), \quad (14)$$

where $\Psi_1(\cdot) : \mathbb{R} \rightarrow \mathbb{R}$ and $\Psi_2(\cdot) : \mathbb{R} \rightarrow \mathbb{R}$ denote the elements of $\mathcal{A}_1(\cdot)$ and $\mathcal{A}_2(\cdot)$ respectively. We define a new variable $g_i(t)$ to facilitate the following analysis, and this variable is formulated as follows:

$$g_i(t) = e_i(t) + \mu \int_0^t \Psi_1(e_i(\tau)) d\tau. \quad (15)$$

Then, the time derivative of $g_i(t)$ (15) can be easily obtained:

$$\dot{g}_i(t) = \dot{e}_i(t) + \mu \Psi_1(e_i(t)). \quad (16)$$

Therefore, substituting (15) and (16) into (14), one can get following simplified dynamics:

$$\dot{g}_i(t) = -\xi \Psi_2(g_i(t)).$$

This formula is the same as the ordinary ZNN model (3), whose properties have already been well studied. According to Lemma 2, if the activation function $\Psi_2(\cdot)$ is odd and monotonically increasing, $g_i(t)$ will converge to zero as the neural network evolves. Since SBP (10) and SFAF (11) all satisfy the condition, NTFZNN model about $g_i(t), \forall i \in \{1, 2, \dots, n^2\}$ is globally stable.

Consider proving the global asymptotic stability of NTFZNN about variable $e_i(t)$, we define an auxiliary Lyapunov function for the i th element of $\mathbf{e}(t)$:

$$L_i(t) = \frac{1}{2} k e_i^2(t) + \frac{1}{2} g_i^2(t),$$

where $k > 0$ is a parameter that particularly specified, and we denote $L_0 = L_i(0) = k e_i^2(0)/2 + g_i^2(0)/2$ with $e_i(0)$ and $g_i(0)$ being the initial value of $e_i(t)$ and $g_i(t)$ respectively. Clearly, L_0 is a known value because $e_i(0)$ and $g_i(0)$ are known. It also holds true that $L_i(t)$ is positive-definite, because $L_i(t) > 0$ for any $e_i(t) \neq 0$ or $g_i(t) \neq 0$; only when $e_i(t) = g_i(t) = 0$ will $L_i(t) = 0$. Then, we calculate the derivative of $L_i(t)$ about time, and the result is as follows:

$$\begin{aligned} \frac{dL_i(t)}{dt} &= k e_i(t) \dot{e}_i(t) + g_i(t) \dot{g}_i(t) \\ &= k e_i(t) [\dot{g}_i(t) - \mu \Psi_1(e_i(t))] - \xi g_i(t) \Psi_2(g_i(t)) \\ &= -k \xi e_i(t) \Psi_2(g_i(t)) - k \mu e_i(t) \Psi_1(e_i(t)) \\ &\quad - \xi g_i(t) \Psi_2(g_i(t)). \end{aligned} \quad (17)$$

To prove the conclusion of Theorem 1, we are going to prove that $L_i(t) \leq 0$ always holds true for $t \in [0, +\infty)$. Firstly, suppose there exists a time instant when $L_i(t) \leq L_0$, therefore following equations can be obtained:

$$\frac{1}{2} k e_i^2(t) \leq L_0 \text{ and } \frac{1}{2} g_i^2(t) \leq L_0.$$

The above inequalities are equivalent to

$$|e_i(t)| \leq \sqrt{2L_0/k} \text{ and } |g_i(t)| \leq \sqrt{2L_0}.$$

Let V_e and V_g represent the domain of $e_i(t)$ and $g_i(t)$ respectively, and we obtain:

$$\begin{aligned} V_e &= \{e_i(t) \in \mathbb{R}, |e_i(t)| \leq \sqrt{2L_0/k}\}, \\ V_g &= \{g_i(t) \in \mathbb{R}, |g_i(t)| \leq \sqrt{2L_0}\}. \end{aligned}$$

For activation functions $\Psi_1(\cdot)$ and $\Psi_2(\cdot)$ with continuous derivative, using the classic mean-value theorem within the domain restricted by V_g , we get:

$$\frac{\Psi_2(g_i(t)) - \Psi_2(0)}{g_i(t) - 0} = \frac{\partial \Psi_2(g_i(\delta))}{\partial g_i} \Big|_{g_i(\delta) \in V_g}. \quad (18)$$

Because $\Psi_2(\cdot)$ is an odd function, $\Psi_2(0) = 0$ holds true. Combining with the monotone increasing feature of $\Psi_2(\cdot)$, we obtain $\partial \Psi_2(g_i(t))/\partial g_i > 0$. Therefore, (18) leads to the following inequality:

$$|\Psi_2(g_i(t))| \leq C_0 |g_i(t)|,$$

where $C_0 = \max\{\partial \Psi_2(g_i(t))/\partial g_i\}_{g_i(t) \in V_g} > 0$ is bounded since V_g is a closed interval and that $\partial \Psi_2(g_i(t))/\partial g_i$ is continuous on this interval. Therefore, we can obtain

$$\begin{aligned} |e_i(t) \Psi_2(g_i(t))| &\leq |e_i(t)| \cdot |\Psi_2(g_i(t))| \\ &\leq C_0 |e_i(t)| \cdot |g_i(t)|. \end{aligned} \quad (19)$$

Similar to the derivation procedure of C_0, C_1 and C_2 can be accordingly obtained by applying the mean-value method:

$$\begin{aligned} |\Psi_1(e_i(t))| &\geq C_1 |e_i(t)|, \\ |\Psi_2(g_i(t))| &\geq C_2 |g_i(t)|, \end{aligned} \quad (20)$$

where C_1 and C_2 are defined as

$$\begin{aligned} C_1 &= \min\{\partial \Psi_1(e_i(t))/\partial e_i\}_{e_i(t) \in V_e} > 0, \\ C_2 &= \min\{\partial \Psi_2(g_i(t))/\partial g_i\}_{g_i(t) \in V_g} > 0. \end{aligned}$$

Combining (17) with (19) and (20), the following inequality can be derived:

$$\begin{aligned}
 \frac{dL_i(t)}{dt} &= -k\xi e_i(t)\Psi_2(g_i(t)) - k\mu e_i(t)\Psi_1(e_i(t)) \\
 &\quad - \xi g_i(t)\Psi_2(g_i(t)) \\
 &\leq k\xi|e_i(t)\Psi_2(g_i(t))| - k\mu e_i(t)\Psi_1(e_i(t)) \\
 &\quad - \xi g_i(t)\Psi_2(g_i(t)) \\
 &\leq k\xi C_0|e_i(t)| \cdot |g_i(t)| - k\mu C_1 e_i^2(t) - \xi C_2 g_i^2(t) \tag{21} \\
 &= -k\left(\sqrt{\mu C_1} e_i(t) - \frac{\xi C_0}{2\sqrt{\mu C_1}} |g_i(t)|\right)^2 \\
 &\quad - k\left(\frac{\xi C_2}{k} - \frac{\xi^2 C_0^2}{4\mu C_1}\right) g_i^2(t).
 \end{aligned}$$

According to the above conclusion of (21), we can guarantee $\dot{L}_i(t) \leq 0$ when $L_i(t) \leq L_0$, provided that

$$\frac{\xi C_2}{k} - \frac{\xi^2 C_0^2}{4\mu C_1} \geq 0 \text{ and } k > 0 \iff 0 < k \leq \frac{4\mu C_1 C_2}{\xi C_0^2}.$$

Obviously we can always find k that satisfies the above condition. Thus, $\dot{L}_i(t) \leq 0$ can be guaranteed when $L_i(t) \leq L_0$. Furthermore, for starting time instant $t = 0$, $L_i(0) \leq L_0$ holds true meaning $\dot{L}_i(0) \leq 0$. Then, we conclude that $L_i(t)$ will be kept in $[0, L_0]$ all the time, i.e. $\dot{L}_i(t) \leq 0$, once k is set properly. Following above process of proof, we have $\dot{L}_i(t) \leq 0$ for any time instant $t \in [0, +\infty)$.

The above analysis have proved the negative semi-definiteness of $\dot{L}_i(t)$. In addition, it follows from the inequality (21) that the upper bound of $\dot{L}_i(t)$ equals to zero only when $e_i(t) = g_i(t) = 0$, meaning $\dot{L}_i(t) < 0$ is true when $e_i(t) \neq 0$ or $g_i(t) \neq 0$. Therefore, $\dot{L}_i(t)$ is negative definite. According to the Lyapunov stability theory in Lemma 1, we finally conclude that all subsystems of (12) are globally stable. Therefore, the proof of Theorem 1 is now complete.

Before obtaining the convergence time upper bound of NTFZNN model (7), we first come to analyze such upper bound of ordinary ZNN model when using two finite-time activation functions SBP (10) and SFAF (11).

Theorem 2. *The error vector $\mathbf{e}(t)$ of the ordinary ZNN model (13) is able to converge to zero in finite time with finite-time convergent activation functions. When SBP (10) is used in $\mathcal{A}(\cdot)$, the convergence time upper bound t_{f1} is $t_{f1} \leq 2|\varrho_{\max}(0)|^{1-p}/(\mu(1-p))$. When SFAF (11) is used in $\mathcal{A}(\cdot)$, the upper bound of convergence time is*

$$t_{f2} = \frac{1}{\alpha_2(1-p)} \ln \frac{\alpha_2|\varrho_{\max}(0)|^{1-p} + \alpha_1}{\alpha_1},$$

where $\alpha_1 = \mu\beta_1 > 0, \alpha_2 = \mu\beta_2 > 0$, and $\varrho(t) \in \mathbb{R}^{n^2}$ denotes the error vector $\mathbf{e}(t)$. In addition, $\varrho_{\max}(t)$ is one element of $\varrho(t)$ which has the largest absolute initial error value, i.e. $|\varrho_{\max}(0)| = \max\{|\varrho_i(0)|, \forall i \in \{1, 2, \dots, n^2\}\}$.

Proof. Consider an auxiliary Lyapunov function candidate $u_i(t) = e_i^2(t)$ for the i th subsystem of (13).

- 1) When SBP (10) is applied in $\mathcal{A}(\cdot)$, the proof of ZNN model (13) about the convergence time upper bound $t_{f1} \leq 2|\varrho_{\max}(0)|^{1-p}/(\mu(1-p))$ can be referred to [37].
- 2) Under the condition that the ordinary ZNN model applies SFAF (11) in $\mathcal{A}(\cdot)$, for calculating the convergence time t_{f2} , we plug (11) into the $\varrho_{\max}(t)$ subsystem of the original design formula (13):

$$\begin{aligned}
 \dot{\varrho}_{\max}(t) &= -\mu(\beta_1 \text{sgn}^p(\varrho_{\max}(t)) + \beta_2 \varrho_{\max}(t)) \\
 &= -\alpha_1 \text{sgn}^p(\varrho_{\max}(t)) - \alpha_2 \varrho_{\max}(t). \tag{22}
 \end{aligned}$$

Solving the above differential equation should be considered under different conditions. First, when $\varrho_{\max}(0) > 0$, (22) leads to the following equality:

$$\dot{\varrho}_{\max}(t) = -\alpha_1(\varrho_{\max}(t))^p - \alpha_2 \varrho_{\max}(t),$$

which is equivalent to a differential equation formed by

$$(\varrho_{\max}(t))^{-p} \frac{d\varrho_{\max}(t)}{dt} + \alpha_2(\varrho_{\max}(t))^{1-p} + \alpha_1 = 0.$$

Defining a auxiliary function $h(t) = (\varrho_{\max}(t))^{1-p}$ and substituting it into above equation, it can be rewritten as

$$\frac{dh(t)}{dt} + (1-p)\alpha_2 h(t) + (1-p)\alpha_1 = 0.$$

Solving the above differential equation, we have

$$h(t) = \left(\frac{\alpha_1}{\alpha_2} + h(0)\right) \cdot \exp((1-p)\alpha_2 t) - \frac{\alpha_1}{\alpha_2},$$

Clearly $\varrho_{\max}(t)$ will decrease to zero at $t = t_{f2}$. Hence, we have $h(t_{f2}) = (\varrho_{\max}(t_{f2}))^{1-p} = 0$. We set $t = t_{f2}$ in above equality, which leads to

$$\begin{aligned}
 t_{f2} &= \frac{1}{\alpha_2(1-p)} \ln \frac{\alpha_2 \varrho_{\max}(0)^{1-p} + \alpha_1}{\alpha_1} \\
 &= \frac{1}{\alpha_2(1-p)} \ln \frac{\alpha_2 |\varrho_{\max}(0)|^{1-p} + \alpha_1}{\alpha_1}.
 \end{aligned}$$

Then, we consider the case when $\varrho_{\max}(0) \leq 0$. Applying the same method as in above analysis and we still get

$$t_{f2} = \frac{1}{\alpha_2(1-p)} \ln \frac{\alpha_2 |\varrho_{\max}(0)|^{1-p} + \alpha_1}{\alpha_1}.$$

Summarizing the conclusions of above two conditions, we can conclude that the proof of Theorem 2 is complete.

From the proof of Theorem 1, we know that the NTFZNN model (7) is built on top of the ordinary ZNN design formula (3). With Theorem 2, the convergence time upper bound of NTFZNN model (7) can now be analyzed.

Theorem 3. *The design formula of NTFZNN model (12) is finite-time convergent, and its convergence time upper bound is*

$$t_{\text{SBP}} \leq \frac{2(\mu + \xi)}{\mu\xi(1-p)} |\varrho_{\max}(0)|^{1-p},$$

when using SBP (10) in $\mathcal{A}_1(\cdot)$ and $\mathcal{A}_2(\cdot)$, where the definition of $\varrho_{\max}(0)$ is the same as in Theorem 2. When SFAF activation function is applied in $\mathcal{A}_1(\cdot)$ and $\mathcal{A}_2(\cdot)$, the upper bound of convergence time is

$$t_{\text{SFAF}} \leq \frac{\mu + \xi}{\mu\xi\beta_2(1-p)} \ln \frac{\beta_2 |\varrho_{\max}(0)|^{1-p} + \beta_1}{\beta_1},$$

where the definition of β_1 and β_2 are the same as in (11).

Proof. 1) Firstly, let us investigate the NTFZNN_{SBP} model. The dynamic formula of NTFZNN model (12) can be reformulated into equation $\dot{\mathbf{g}}(t) = -\xi \mathcal{A}_2(\mathbf{g}(t))$, where $\mathbf{g}(t) = \mathbf{e}(t) + \mu \int_0^t \mathcal{A}(\mathbf{e}(\tau)) d\tau \in \mathbb{R}^{n^2}$. Evidently this dynamic is identical with the formula of the ordinary ZNN formula (13). Then according to the conclusion of Theorem 2, $\mathbf{g}(t)$ should converge to zero in finite-time t_1 as

$$t_1 \leq \frac{2}{\xi(1-p)} |\varrho_{\max}(0)|^{1-p},$$

where $\varrho_{\max}(0) = \max\{|g_i(0)|\} = \max\{|e_i(0)|\}, \forall i \in \{1, 2, \dots, n^2\}$. After time period t_1 , $\mathbf{g}(t)$ stays at its equilibrium point, meaning

$\dot{\mathbf{g}}(t) = \mathbf{0}$. The error vector then satisfies $\dot{\mathbf{e}}(t) = -\mu \mathcal{A}_1(\mathbf{e}(t))$. Again, this equation is the same as the ordinary ZNN model (13). It is known that for the NTFZNN model (12), the absolute value $|e_i(t)|$ is always decreasing until it reaches zero, thus $|e_i(t_1)| \leq |e_i(0)|$, $\forall i \in \{1, 2, \dots, n^2\}$ holds true. According to the Theorem 2, $\mathbf{e}(t)$ must converge to zero in time t_2 :

$$t_2 \leq \frac{2}{\mu(1-p)} |Q_{\max}(0)|^{1-p}.$$

In summary, $\mathbf{e}(t)$ of NTFZNN_{SBP} eventually converges to zero after two time periods, whose time upper bound are t_1 and t_2 respectively. We can now conclude that the NTFZNN_{SBP} model for time-varying Lyapunov equation converges in finite time t_{SBP} :

$$t_{\text{SBP}} = t_1 + t_2 \leq \frac{2(\mu + \xi)}{\mu\xi(1-p)} |Q_{\max}(0)|^{1-p}.$$

The first part of Theorem 3 has been proved.

2) Considering the NTFZNN_{SFAF} model, similar to the proof of first part of Theorem 3, its convergence process can still be split into two stages with the aid of auxiliary function $\mathbf{g}(t) = \mathbf{e}(t) + \mu \int_0^t \mathcal{A}(\mathbf{e}(\tau)) d\tau$. Following Theorem 2, in first stage, we can derive that $\mathbf{g}(t)$ converges to zero in finite time t_3 :

$$t_3 = \frac{1}{\xi\beta_2(1-p)} \ln \frac{\beta_2 |Q_{\max}(0)|^{1-p} + \beta_1}{\beta_1}.$$

Then, in the second stage, $\mathbf{e}(t)$ will converge to zero in finite time t_4 as

$$t_4 \leq \frac{1}{\mu\beta_2(1-p)} \ln \frac{\beta_2 |Q_{\max}(0)|^{1-p} + \beta_1}{\beta_1}.$$

Finally, we come to a conclusion that NTFZNN_{SFAF} is finite-time convergent with convergence time upper bound being

$$t_{\text{SFAF}} = t_3 + t_4 \leq \frac{\mu + \xi}{\mu\xi\beta_2(1-p)} \ln \frac{\beta_2 |Q_{\max}(0)|^{1-p} + \beta_1}{\beta_1}.$$

The proof of Theorem 3 is now complete.

4.2. Robustness analysis

In this subsection, we are going to investigate the noise suppression ability of NTFZNN model (12). Consider an unknown additive noise $\Delta_N(t) \in \mathbb{R}^{n^2}$, which is added to the vector form of the NTFZNN model, forming the following inherent dynamics:

$$\dot{\mathbf{e}}(t) = -\mu \mathcal{A}_1(\mathbf{e}(t)) - \xi \mathcal{A}_2 \left(\mathbf{e}(t) + \mu \int_0^t \mathcal{A}_1(\mathbf{e}(\tau)) d\tau \right) + \Delta_N(t). \quad (23)$$

To lay the basis for the following analysis in this subsection, the above Eq. (23) is called the dynamics of the noise polluted NTFZNN model.

Theorem 4. *If the additive noise $\Delta_N(t)$ is constant, then residual error $\mathbf{e}(t)$ of the noise polluted NTFZNN model (23) globally converges to $\mathbf{0}$ with the neural network evolving.*

Proof. Because the noise $\Delta_N(t)$ is constant, we denote it by Δ_N , and the i th subsystem of (23) leads to

$$\dot{e}_i(t) = -\mu \Psi_1(e_i(t)) - \xi \Psi_2 \left(e_i(t) + \mu \int_0^t \Psi_1(e_i(\tau)) d\tau \right) + \delta_i, \quad (24)$$

where δ_i is the i th element of Δ_N . We introduce a auxiliary function $g_i(t)$ defined in (15). Substituting $g_i(t)$ and (16) into (24) leads to

$$\dot{g}_i(t) = -\xi \Psi_2(g_i(t)) + \delta_i.$$

The following Lyapunov function candidate is designed to investigate the stability of (24):

$$v_i(t) = (\xi \Psi_2(g_i(t)) - \delta_i)^2 / 2.$$

Since $v_i(t) \geq 0$ and $v_i(t) = 0$ only when $\dot{g}_i(t) = 0$, $v_i(t)$ is clearly a positive definite function. We calculate its time derivative as

$$\begin{aligned} \frac{dv_i}{dt} &= (\xi \Psi_2(g_i(t)) - \delta_i) \xi \frac{\partial \Psi_2(g_i(t))}{\partial g_i} \dot{g}_i(t) \\ &= -\xi \frac{\partial \Psi_2(g_i(t))}{\partial g_i} (\xi \Psi_2(g_i(t)) - \delta_i)^2. \end{aligned}$$

The conclusion of $\partial \Psi_2(g_i(t)) / \partial g_i > 0$ can be easily derived from activation functions' odd and monotone increasing property. Thus, $\dot{v}_i(t) \leq 0$, and $\dot{v}_i(t) = 0$ if and only if $\xi \Psi_2(g_i(t)) - \delta_i = 0$, implying that $\dot{v}_i(t)$ is negative definite. Now, we obtain that $v_i(t)$ always converges to 0 according to Lemma 1. With $v_i(t)$ converging to zero, $\xi \Psi_2(g_i(t)) - \delta_i$ converges to zero too, i.e., $\lim_{t \rightarrow +\infty} \dot{g}_i(t) = -\xi \Psi_2(g_i(t)) + \delta_i = 0$.

Let us take $\dot{g}_i(t) = \dot{e}_i(t) + \xi \Psi_1(e_i(t))$ into account, since $\lim_{t \rightarrow +\infty} \dot{g}_i(t) = 0$, it will reduce to following equality with $t \rightarrow +\infty$:

$$\dot{e}_i(t) = -\xi \Psi_1(e_i(t)).$$

The above equality is the same as i th subsystem of the ordinary ZNN model (13). Obviously $e_i(t)$ will converge to zero with $t \rightarrow +\infty$ according to the Lemma 2.

Finally, combining the above analyses together, we come into conclusion that NTFZNN model (12) is globally stable even facing with unknown constant additive noise. Theorem 4 has now been proved.

Results of Theorem 4 have shown that polluted NTFZNN model (23) can still converge to the accurate solution even with constant additive noises, which is excellent noise resistance ability. However, time-varying unknown additive noises are more common than specific noise and thus we will investigate them in the following theorem.

Theorem 5. *If the unknown time-varying additive noise $\Delta_N(t)$ in the disturbed NTFZNN model (23) is assumed to have continuous time derivative and its time derivative is bounded at any time instant $t \geq 0$. Then, the computation error $\|\mathbf{e}(t)\|_2$ of the disturbed NTFZNN model (23) converges to the interval $[0, n|\dot{\delta}_{\max}(t)| / (\mu\xi\rho)]$ when $t \rightarrow +\infty$. Moreover, $\delta_i(t)$ is the i th element of $\Delta_N(t)$ with $|\dot{\delta}_{\max}(t)|$ being the upper bound of $|\dot{\delta}_i(t)|$, $\rho_i = |\Psi_1(e_i(t))| / |e_i(t)| \geq 1$ and $\rho = \min\{\rho_i | i \in 1, 2, \dots, n^2\}$.*

Proof. We consider an auxiliary function $u_i(t) = g_i^2(t) / 2 = |g_i(t)|^2 / 2$ for the i th element of $\mathbf{g}(t) = \mathbf{e}(t) + \mu \int_0^t \mathcal{A}(\mathbf{e}(\tau)) d\tau$, the following dynamics can be easily obtained from i th subsystem of (23):

$$\dot{g}_i(t) = -\xi \Psi_2(g_i(t)) + \delta_i(t). \quad (25)$$

Therefore, we take the time derivative of $u_i(t)$ as follows:

$$\dot{u}_i(t) = \dot{g}_i(t)g_i(t) = (-\xi \Psi_2(g_i(t)) + \delta_i(t))g_i(t).$$

Considering that $\Psi_2(g_i(t))g_i(t) \geq 0$ holds true for any $g_i(t)$, we have $\dot{u}_i(t) \leq 0$ when $\delta_i(t)g_i(t) \leq 0$, meaning $|g_i(t)| = \sqrt{u_i(t)}$ will not increase. Particularly, in the case of $\delta_i(t)g_i(t) \leq 0$ if $|g_i(t)| \neq 0$, it yields from (25) that $|g_i(t)|$ always decreases whenever $\delta_i(t) = 0$ or $\delta_i(t) \neq 0$. In other cases when $\delta_i(t)g_i(t) > 0$, $|g_i(t)|$ may increase, which leads to the decrease of $|\xi \Psi_2(g_i(t)) + \delta_i(t)|$. However, this decreasing process stops when $-\xi \Psi_2(g_i(t)) + \delta_i(t) = 0$, which makes $\dot{u}_i(t) = 0$ again. Thus, it is obvious that when $t \rightarrow +\infty$, $|g_i(t)|$ is bounded by

$$-|\Psi_2^{-1}(\delta_i(t)/\xi)| \leq |g_i(t)| \leq |\Psi_2^{-1}(\delta_i(t)/\xi)|,$$

where $\Psi_2^{-1}(\cdot)$ is the inverse function of $\Psi_2(\cdot)$. Because $|\Psi_2(x)| \geq |x|$, i.e., $|\Psi_2^{-1}(x)| \leq |x|$ is true for the activation functions used in this paper, the bound of $|g_i(t)|$ can be reformulated as follows:

$$\begin{aligned} -|\delta_i(t)/\xi| &\leq |g_i(t)| \leq |\delta_i(t)/\xi|, \\ -|\delta_i(t)/\xi| &\leq g_i(t) \leq |\delta_i(t)/\xi|. \end{aligned} \tag{26}$$

We now come to prove that $\mu\Psi_1(e_i(t))$ tends to fall into the interval $\mu\Psi_1(e_i(t)) \in [-|\delta_i(t)/\xi, |\delta_i(t)/\xi]$ when $t \rightarrow +\infty$. Supposing there exists any time instant $t_1 > 0$ such that $g_i(t_1) = e_i(t_1) + \mu \int_0^{t_1} \Psi_1(e_i(\tau))d\tau = S_1$ and $\mu\Psi_1(e_i(t_1)) \notin [-|\delta_i(t_1)/\xi, |\delta_i(t_1)/\xi]$.

Without loss of generality, we assume $\mu\Psi_1(e_i(t_1)) > |\delta_i(t_1)/\xi > 0$. If $e_i(t)$, starting from $e_i(t_1)$, keeps $\mu\Psi_1(e_i(t)) > |\delta_i(t)/\xi$ in the following time period, then after time period t_2 we have $g_i(t_1 + t_2) = e_i(t_1 + t_2) + \mu \int_0^{t_1+t_2} \Psi_1(e_i(\tau))d\tau = S_2$. Calculating the difference between S_1 and S_2 , we have

$$\begin{aligned} S_2 - S_1 &= (e_i(t_1 + t_2) - e_i(t_1)) + \mu \int_0^{t_1+t_2} \Psi_1(e_i(\tau))d\tau \\ &\quad - \mu \int_0^{t_1} \Psi_1(e_i(\tau))d\tau \\ &= (e_i(t_1 + t_2) - e_i(t_1)) + \mu \int_{t_1}^{t_1+t_2} \Psi_1(e_i(\tau))d\tau \\ &\geq \mu \int_{t_1}^{t_1+t_2} \Psi_1(e_i(\tau))d\tau - e_i(t_1). \end{aligned} \tag{27}$$

Besides, from above analysis, we obtain

$$\begin{aligned} &|\delta_i(t_1 + t_2)/\xi| - S_1 \\ &= |\delta_i(t_1)/\xi + [\delta_i(t_1 + t_2)/\xi - \delta_i(t_1)/\xi]| - S_1 \\ &\leq |\delta_i(t_1)/\xi| + |\delta_i(t_1 + t_2)/\xi - \delta_i(t_1)/\xi| - S_1 \\ &= |\delta_i(t_1)/\xi| + \left| \int_{t_1}^{t_1+t_2} (\dot{\delta}_i(\tau)/\xi)d\tau \right| - S_1 \\ &\leq |\delta_i(t_1)/\xi| + \int_{t_1}^{t_1+t_2} |\dot{\delta}_i(\tau)/\xi|d\tau - S_1. \end{aligned} \tag{28}$$

It follows from (27) and (28) that:

$$S_2 - |\delta_i(t_1 + t_2)/\xi| \geq \int_{t_1}^{t_1+t_2} (\mu\Psi_1(e_i(\tau)) - |\dot{\delta}_i(\tau)/\xi|)d\tau - (|\delta_i(t_1)/\xi| + e_i(t_1) + S_1).$$

From previous assumption, $\mu\Psi_1(e_i(t)) - |\dot{\delta}_i(t)/\xi| > 0$ holds true for $t \in [t_1, t_1 + t_2]$ and $|\delta_i(t_1)/\xi| + e_i(t_1) + S_1$ is an given infinite value for any given t_1 . In addition, inequality (26) implies that $S_2 = g_i(t_1 + t_2) \leq |\delta_i(t_1 + t_2)/\xi|$. Therefore, we have

$$\int_{t_1}^{t_1+t_2} (\mu\Psi_1(e_i(\tau)) - |\dot{\delta}_i(\tau)/\xi|)d\tau \leq (|\delta_i(t_1)/\xi| + e_i(t_1) + S_1). \tag{29}$$

It is worth pointing out that the left side of (29) is always increasing with the increasing of time t_2 , while the right side of (29) is a finite fixed value. Hence, when $t_2 \rightarrow +\infty$, we conclude that $\lim_{t \rightarrow +\infty} (\mu\Psi_1(e_i(t)) - |\dot{\delta}_i(t)/\xi|) = 0$, i.e., $\lim_{t \rightarrow +\infty} \mu\Psi_1(e_i(t)) = |\dot{\delta}_i(t)/\xi|$. For the case when $\mu\Psi_1(e_i(t_1)) < -|\delta_i(t_1)/\xi < 0$ and $\mu\Psi_1(e_i(t)) < -|\dot{\delta}_i(t)/\xi$ keeps true in the following time period, we can obtain $\lim_{t \rightarrow +\infty} \mu\Psi_1(e_i(t)) = -|\dot{\delta}_i(t)/\xi|$ in a similar way.

Combining the above analysis results, even if there exists time instant t such that $\mu\Psi_1(e_i(t)) \notin [-|\delta_i(t)/\xi, |\delta_i(t)/\xi]$, $\mu\Psi_1(e_i(t))$ still converge to interval $[-|\dot{\delta}_i(t)/\xi, |\dot{\delta}_i(t)/\xi]$ when $t \rightarrow +\infty$. This conclusion shows that $e_i(t)$ converges to $[-|\dot{\delta}_i(t)/(\mu\xi\rho_i), |\dot{\delta}_i(t)/(\mu\xi\rho_i)]$ for $t \rightarrow +\infty$. Furthermore, $\|\mathbf{e}(t)\|_2$ satisfies

$$0 \leq \|\mathbf{e}(t)\|_2 = \sqrt{\sum_{i=1}^{n^2} e_i^2(t)} \leq n|e_{\max}(t)|,$$

where $|e_{\max}(t)|$ has the largest value among $|e_i(t)|, \forall i \in \{1, 2, \dots, n^2\}$. Finally, we are able to conclude that the

computation error $\|\mathbf{e}(t)\|_2$ of perturbed NTFZNN model (23) converges to interval $[0, n|\dot{\delta}_{\max}(t)/(\mu\xi\rho)]$ with $t \rightarrow +\infty$. Theorem 5 has now been proved.

Remark 1. As illustrated in Theorem 5, when facing with various kinds of time-varying additive noises, the steady state error $\|\mathbf{e}(t)\|_2$ of the perturbed NTFZNN model (23) is still bounded as long as the noises have bounded time derivatives. Considering that even if the additive noises do not satisfy such requirement, most of them can be approximated by Fourier series which satisfy our requirement. Therefore our conclusion in Theorem 5 actually has shown NTFZNN model's strong robustness against wide range of additive noises.

5. Simulative verification and comparison

Theoretical analyses in previous sections have laid a solid theoretical foundation for the NTFZNN model. In this section, we mainly focus on validating the convergence and noise suppress abilities of the NTFZNN model when applied to time-varying Lyapunov equation problem solving. Without loss of generality, the coefficients in the time-varying Lyapunov problem (1) are selected as the following form

$$M(t) = \begin{bmatrix} -1 - \frac{1}{2} \cos(3t) & \frac{1}{2} \sin(3t) \\ \frac{1}{2} \sin(3t) & -1 + \frac{1}{2} \cos(3t) \end{bmatrix},$$

$$Q(t) = \begin{bmatrix} \sin(3t) & \cos(3t) \\ -\cos(3t) & \sin(3t) \end{bmatrix}.$$

Because the coefficient matrix $M(t)$ and $Q(t)$ are given, we can calculate out the theoretical solution $A(t)$ of Lyapunov Eq. (1), and the ij th element $A_{ij}(t)$ of matrix $A(t)$ are written as follows:

$$\begin{aligned} A_{11}(t) &= -\frac{1}{3} \sin(3t)(\cos(3t) - 2), \\ A_{12}(t) &= -\frac{1}{6} (2 \cos(3t) - 1)(\cos(3t) + 2), \\ A_{21}(t) &= -\frac{1}{6} (2 \cos(3t) + 1)(\cos(3t) - 2), \\ A_{22}(t) &= \frac{1}{3} \sin(3t)(\cos(3t) + 2), \end{aligned}$$

where the correctness of $A(t)$ can be validated by substituting it into the problem (1). Therefore, we use $A(t)$ to verify the model accuracy.

In the ideal environment without internal and external disturbance, both NTFZNN_{SBP} and NTFZNN_{SFAF} can converge to the accurate solution of Lyapunov equation in finite time, which have been proved in Theorem 3. For experimental purpose, in initial error matrix $E(0) \in \mathbb{R}^{2 \times 2}$, every element $e_{ij}(0) \in E(0)$ is random generated and is bounded by $|e_{ij}(0)| \in [0, 2]$. Other design parameters are selected as $\mu = 2, \xi = 1$ in NTFZNN models, $p = 0.4$ in $\psi_{SFAF}(\cdot)$ and $\psi_{SBP}(\cdot)$ activation functions, $\beta_1 = \beta_2 = 1$ in $\psi_{SFAF}(\cdot)$. Fig. 1 shows that, the residual error $\|M^T(t)X(t) + X(t)M(t) + Q(t)\|_F = \|\mathbf{e}(t)\|_2$ of two NTFZNN models starting from the same original state converges to zero quickly and in finite time. It is worth mentioning that we can calculate the convergence time upper bound of these NTFZNN models according to the Theorem 3, which is derived as follows:

$$t_{SBP} \leq \frac{2(2+1)}{2(1-0.4)} 2^{(1-0.4)} \leq 7.58 \text{ s},$$

$$t_{SFAF} \leq \frac{2+1}{2(1-0.4)} \ln \frac{2^{(1-0.4)}+1}{1} \leq 2.31 \text{ s},$$

where t_{SBP} , and t_{SFAF} are theoretical upper bound of convergence time of NTFZNN_{SBP} and NTFZNN_{SFAF}, respectively. It can be seen in Fig. 1 that $\|\mathbf{e}(t)\|_2$ of these models takes about 3.5 s and 2.3 s to reach zero, which obviously satisfies the conclusion. What's more, Fig. 2 illustrates the output transients of the NTFZNN_{SFAF} model, where the red dotted line denotes theoretical solution and the blue

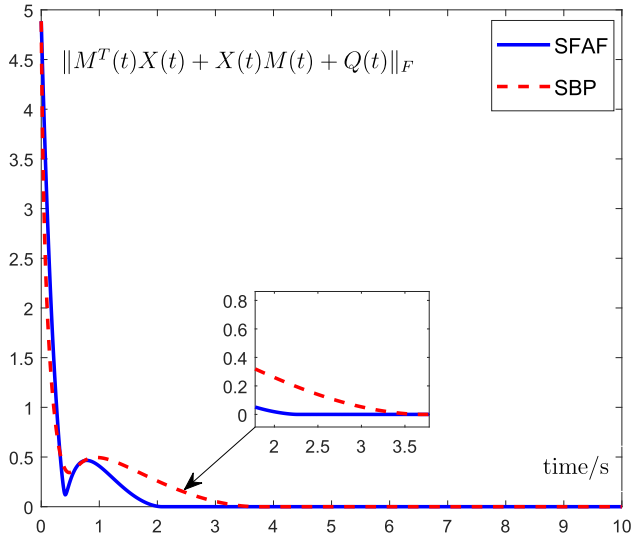


Fig. 1. Trajectory of residual error $\|M^T(t)X(t) + X(t)M(t) + Q(t)\|_F$ synthesized by NTFZNN model (7) when using SFAF (blue solid line) and SBP (red dotted line) activation functions. (For interpretation of the references to color in this figure legend, the reader is referred to the web version of this article.)

solid line represents the neural network solution. Clearly, the NTFZNN_{SFAF} model tracks the accurate solution quickly and precisely. Besides, the performance of NTFZNN_{SBP} is similar and is thus omitted.

Next, we come to examine the performance of the perturbed NTFZNN model (23). This time we choose $\psi_{SFAF}(\cdot)$ as the activation function used in $\Psi_1(\cdot)$ and $\Psi_2(\cdot)$ because its performance is better. We have also conducted simulations using the ordinary ZNN model

(4) and the NTZNN model (9) as contrast group, where $\mathcal{A}(\cdot)$ in the ZNN model uses $\psi_{SFAF}(\cdot)$ too. Other parameters are set to be $p = 0.4$, $\mu = 3$, $\zeta = 2$ and $\beta_1 = \beta_2 = 1$. When facing with constant noise $\delta_i(t) = 2$, the residual error trajectories of neural network models are depicted in Fig. 3, which shows that the residual errors $\|e(t)\|_2$ of the NTFZNN and NTZNN models decrease to zero with time, while the ordinary ZNN model's stays at a very large level. These facts imply the NTFZNN and NTZNN models can converge to the theoretical solution but the ordinary ZNN model can not. This phenomenon also verifies the conclusion of Theorem 4. In order to demonstrate the superior noise toleration ability of the NTFZNN model, we set the additive noise to be linear type $\delta_i(t) = 2t$, the design parameter are set to be $\mu = 5$, $\zeta = 2$ accordingly, and the simulative results are shown in Fig. 4. As demonstrated in Fig. 4, even under such huge perturbation, the NTFZNN model still maintains its effectiveness with very small stable residual error $\|e(t)\|_2$ near zero, while the stable residual error of the NTZNN model is about 2 and the ordinary ZNN model with even larger increasing error. Furthermore, the convergence speed of the NTFZNN model is much faster than the NTZNN model in both Fig. 3 and Fig. 4, because the latter one is lack of nonlinear activation functions.

Theorem 5 illustrates that in the face of unknown nonstationary additive noise, the stable residual error $\|e(t)\|_2$ of the NTFZNN model is bounded and predictable given that the noise's time derivative is bounded. This conclusion shows the superiority of the NTFZNN model under noise polluted condition, and thus we have designed two simulative experiments to verify Theorem 5. Note that in these two experiments, we use $f(x) = x$ as activation function in $\Psi_1(\cdot)$ and $\Psi_2(\cdot)$ for analyze convenience, i.e., $\rho = 1$. Firstly, design parameters are set as $\mu = 2$, $\zeta = 1$ and the noise $\delta_i(t)$ changes from $0.5t$, t to $2t$, thus the steady-state residual error upper bound changes from 2, 1 to 0.5 in Theorem 5, which matches

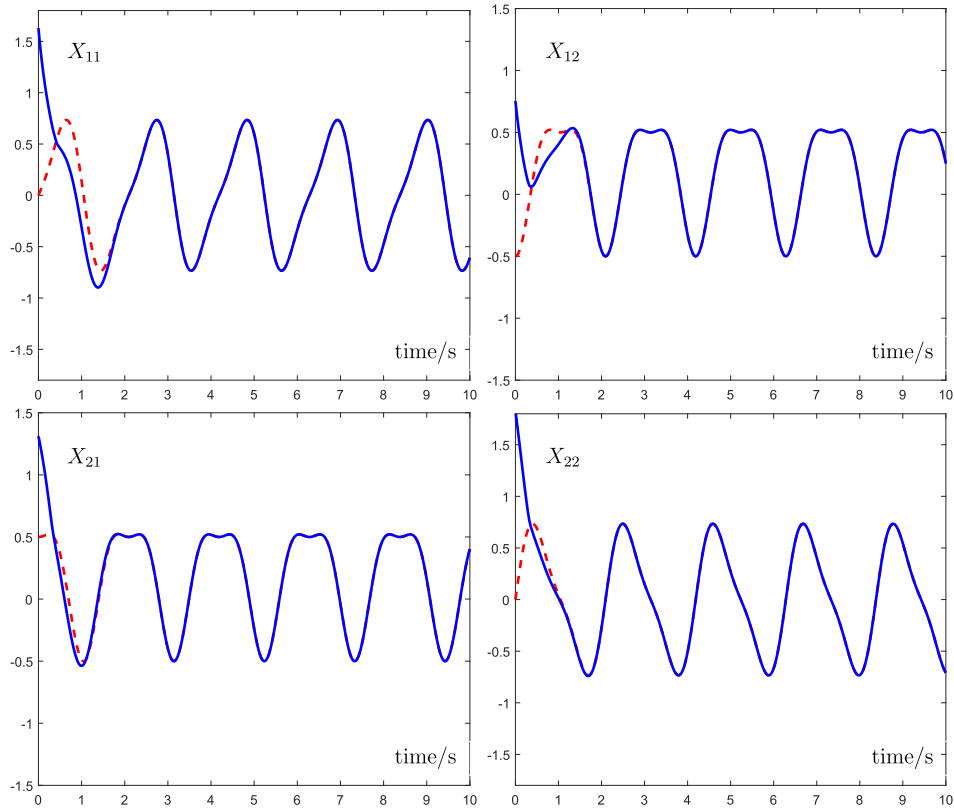


Fig. 2. Elements of neural state $X(t)$ synthesized by NTFZNN model (7) using SFAF (11) activation function.

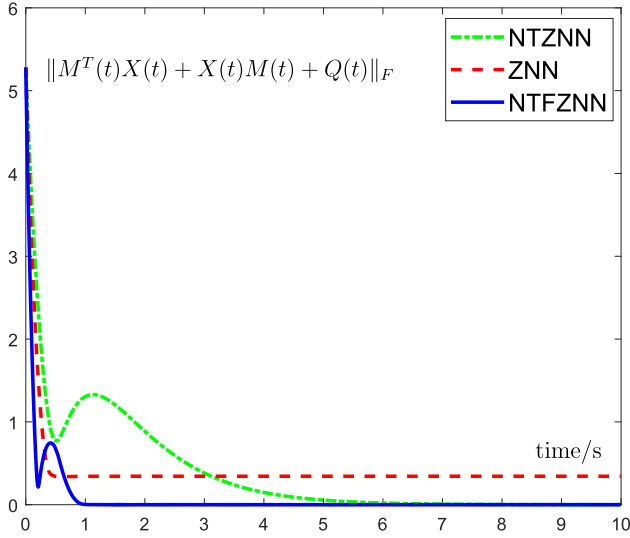


Fig. 3. Computing time-varying Lyapunov equation problem in the presence of additive constant noise $\delta_i(t) = 2$, using the NTFZNN model (blue solid line), the NTZNN model (green dotted line) and the ordinary ZNN model (red dotted line). (For interpretation of the references to color in this figure legend, the reader is referred to the web version of this article.)

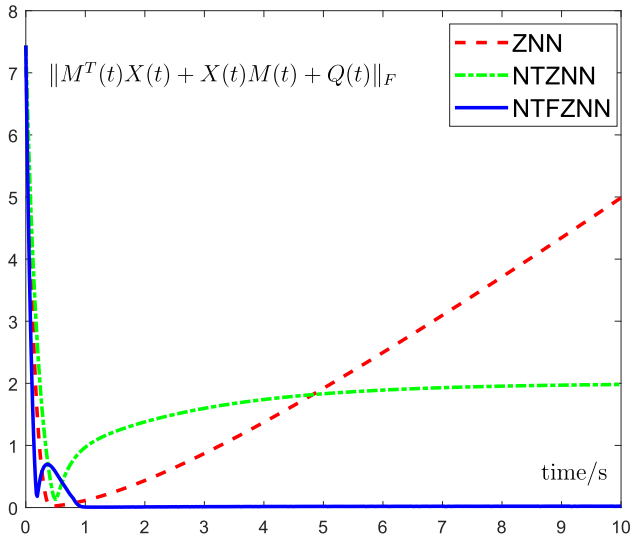


Fig. 4. Computing time-varying Lyapunov equation problem facing additive increasing noise $\delta_i(t) = 2t$, using NTFZNN model (blue solid line), NTZNN model (green dotted line) and the ordinary ZNN model (red dotted line). (For interpretation of the references to color in this figure legend, the reader is referred to the web version of this article.)

the results shown in Fig. 5(a) perfectly. In the second experiment, $\delta_i(t)$ is fixed to be $2t$ while design parameters are set as $\mu = 2$, $\xi = 1$, $\mu = 4$, $\xi = 1$ to $\mu = 4$, $\xi = 2$. As depicted in Fig. 5 (b), the stable $\|\mathbf{e}(t)\|_2$ changes from about 1, 0.5 to 0.25, validating the Theorem 5 again. Obviously, the robustness of the NTFZNN model is excellent. Moreover, the convergence speed and noise suppression ability can be improved through increasing μ , ξ and adopting better nonlinear activation functions.

6. Application to perturbed mobile manipulator control

In the previous section, we have used NTFZNN model (7) to solve the nonstationary Lyapunov equation problem and we only

solve a slightly simple Lyapunov equation for concise demonstration. However, to validate the efficacy of our proposed NTFZNN model on applying to the real-world task, we introduce a mobile manipulator to test it as in [13,38,39]. The robot manipulator is a wheeled mobile manipulator, whose model and mechanical structure can be seen in [40]. Furthermore, one can learn from [40] that the kinematics model of this robot manipulator can be formulated as following equation:

$$\mathbf{r}(t) = \mathbf{y}(\Theta(t)) \in \mathbb{R}^k,$$

where $\Theta(t) = [\phi^T(t), \theta^T(t)]^T \in \mathbb{R}^{n+2}$ represents the angle vector that consists of the mobile platform angle vector $\phi(t) = [\phi_L(t), \phi_R(t)]^T$ and the manipulator angle vector $\theta(t) = [\theta_1(t), \dots, \theta_n(t)]^T$. Besides, $\mathbf{r}(t) = [r_x(t), r_y(t), r_z(t)]^T$ denotes the position of end-effector in Cartesian space, and $\mathbf{y}(\cdot)$ denotes a smooth function mapping $\Theta(t)$ to $\mathbf{r}(t)$ in nonlinear behavior.

Following the inverse kinematic control method and the NTFZNN model, the dynamic equation used to accomplish the tracking control task of this mobile manipulator can be obtained as

$$J(\Theta(t))\dot{\Theta}(t) = \dot{\mathbf{r}}(t) - \mu\Psi_1(\mathbf{e}(t)) - \xi\Psi_2\left(\mathbf{e}(t) + \mu \int_0^t \mathbf{e}(\tau)d\tau\right),$$

where $J(\Theta(t)) = \partial\mathbf{y}(\Theta(t))/\partial\Theta \in \mathbb{R}^{m \times (n+2)}$, $\mathbf{e}(t) = \mathbf{r}(t) - \mathbf{y}(\Theta(t))$ is the error vector of end-effector position. Considering that the most important advantage of the NTFZNN model is its ability to work reliably even under large noise condition, we inject an increasing noise $\delta(t) = 2t$ to above dynamics:

$$J(\Theta(t))\dot{\Theta}(t) = \dot{\mathbf{r}}(t) - \mu\Psi_1(\mathbf{e}(t)) - \xi\Psi_2(\mathbf{e}(t) + \mu \int_0^t \mathbf{e}(\tau)d\tau) + \delta(t). \quad (30)$$

In the simulation, we set $\mu = 100$, $\xi = 5$, $\Theta(0) = [0, 0, \pi/3, \pi/12, \pi/12, \pi/12, \pi/12, \pi/12]$. The tracking duration is 10 s and the activation function we use is SFAP (11) with $p = 0.5$ and $\beta_1 = \beta_2 = 1$. Under this condition, we use the perturbed manipulator control dynamic (30) to track a Four-leaf clover shape path and the results are shown in Figs. 6 and 7(a). Fig. 6 illustrates the whole tracking process of mobile manipulator controlled by model (30), where Fig. 6(a) plots in 3D view angle and Fig. 6(b) plots top graph of the process. Evidently, although under large linear noise, the model accomplish the tracking task well, this can be further verified in Fig. 7(a) which depicts the desired path and actual end-effector trajectory. Particularly, in Fig. 7(a), we find that the position error of the path is about the level of 10^{-5} m on all three axes under such large noise perturbation.

It has been demonstrated in Fig. 4 that the NTFZNN model (12) outperforms the ordinary ZNN model (13) and the NTZNN model (9) when facing time-varying additive noises. Therefore, it is necessary to verify whether the NTFZNN model (12) still outperforms above other two models in the perturbed robotic tracking task. Similar to constructing the perturbed NTFZNN model based robot control model (30), we have the perturbed NTZNN model based robot control model as $J(\Theta(t))\dot{\Theta}(t) = \dot{\mathbf{r}}(t) - \mu\mathbf{e}(t) - \xi \int_0^t \mathbf{e}(\tau)d\tau + \delta(t)$ and the perturbed ordinary ZNN model based robot control model as $J(\Theta(t))\dot{\Theta}(t) = \dot{\mathbf{r}}(t) - \mu\Psi_1(\mathbf{e}(t)) + \delta(t)$. Then in above three robot control models, all activation functions $\Psi_1(\cdot)$, $\Psi_2(\cdot)$ are set to be SFAP (11) while other parameters are set as $\delta_i(t) = 2 * t - \sin(t)$, $p = 0.5$, $\beta_1 = \beta_2 = 1$, $\xi = 1$ and $\mu = 10, 11, \dots, 20$. With above settings and starting from the same initial condition $\Theta(0)$, the three perturbed robot control model are used to track a desired path which is the same as in above experiment. Note that the Maximum Steady State Position Error (MSSPE) as a new evaluation index is adopted in the simulation results of Fig. 8. Besides, the MSSPE is defined as $\max\{\text{err}_p(t)\}$, $\forall t \in [7, 10]$ s. From Fig. 8, evi-

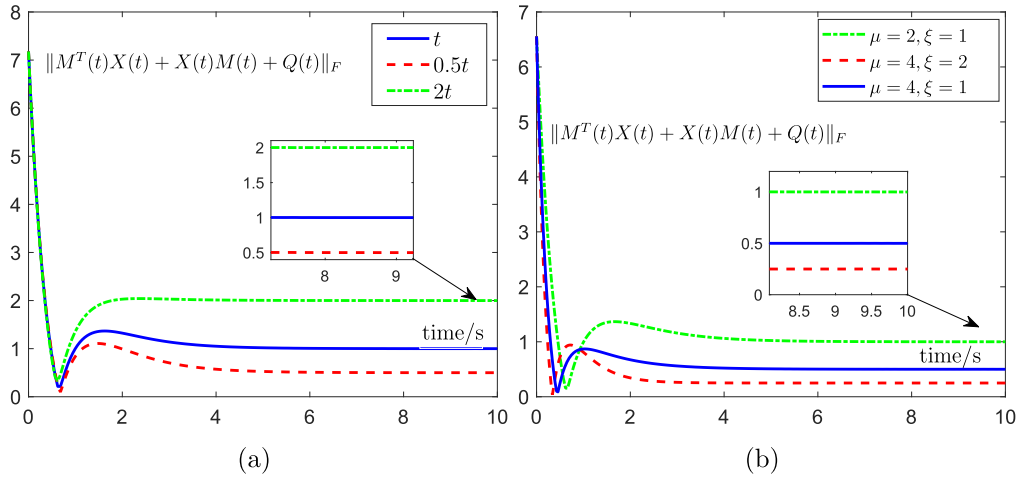


Fig. 5. Residual error $\|M^T(t)X(t) + X(t)M(t) + Q(t)\|_F$ generated by perturbed NTFZNN model (23). (a) Under different additive noise $\delta_i(t) = 0.5t$ (blue solid line), $\delta_i(t) = t$ (red dotted line) and $\delta_i(t) = 2t$. (b) Using different design parameters μ and ξ . (For interpretation of the references to color in this figure legend, the reader is referred to the web version of this article.)

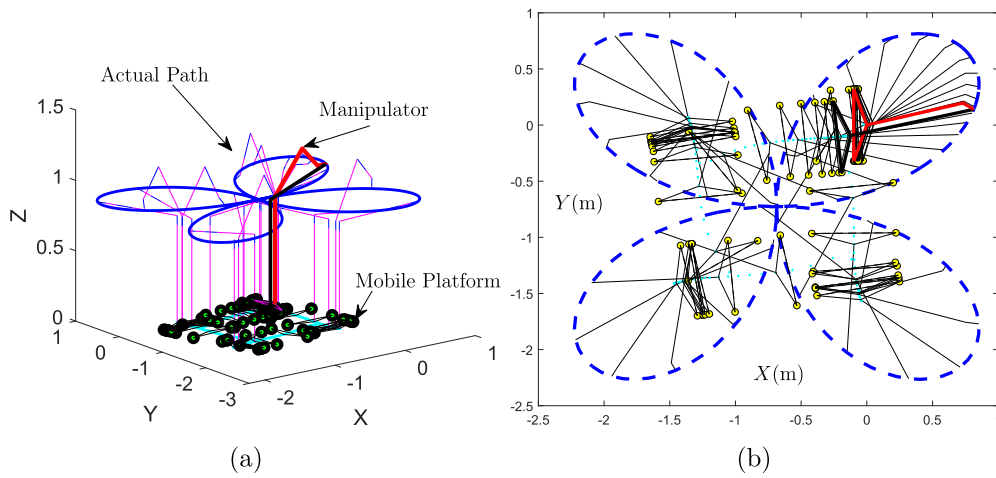


Fig. 6. Results of tracking Four-leaf clover path using the perturbed NTFZNN model (30) controlled the mobile manipulator. (a) Complete tracking movement process. (b) Top view of according tracking trajectories.

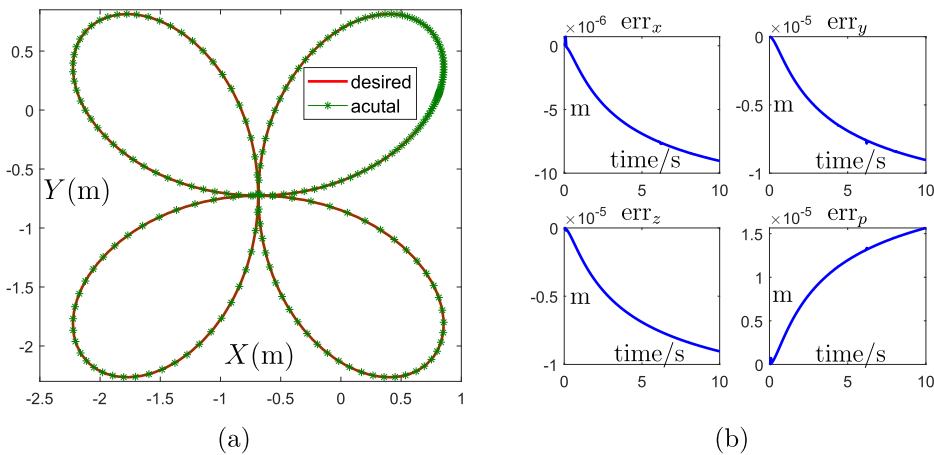


Fig. 7. Profiles produced by the perturbed NTFZNN model (30) controlled mobile manipulator during tracking task. (a) Desired path (red solid line) and actual path (green dots). (b) Tracking position level error along three axes and as a whole in Cartesian space.

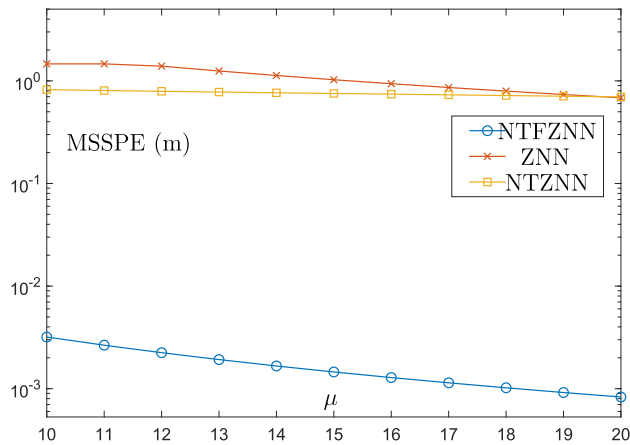


Fig. 8. MSSPE trajectories of three perturbed robot manipulator control models which are based on the NTFZNN, NTZNN or ZNN models during tracking tasks and with different μ .

dently, the perturbed NTFZNN model based robot control model's MSSPEs are always more than 100 times smaller than that of other two perturbed robot control models, which shows that the NTFZNN model works much better than the NTZNN model (9) and the ordinary ZNN model (13) in perturbed robot manipulator control.

In summary, the above simulation results have shown that the NTFZNN based robot control model (30) can handle the mobile manipulator tracking task well in heavily perturbed environment.

7. Conclusion

In order to accelerate the convergence speed to finite time as well as to perform reliably even when there exists various types of internal and external noise, a novel Noise-Tolerance Finite-time convergent ZNN (NTFZNN) model is established to deal with the time-varying Lyapunov equation. Equipped with two finite-time convergent activation functions, the advanced properties of the NTFZNN model are firstly proved theoretically. Numerical simulative experiments have validated that NTFZNN is able to converge to the accurate solution of time-varying Lyapunov equations. It has also been proved and validated by numerical simulations that when the additive noise has bounded time derivative, the stable residual error of perturbed NTFZNN is bounded and can be computed out. Furthermore, the design method of NTFZNN is adopted to control a wheeled mobile manipulator under increasing additive noise in real-time, which successfully tracks the desired path with high accuracy. Future work can be finding ways to further enhance convergence speed of the NTFZNN model. Transforming the NTFZNN model into discrete model and exploiting it to deal with more practical applications also worth in-depth research.

CRedit authorship contribution statement

Zeshan Hu: Data curation, Writing - original draft, Visualization. **Kenli Li:** Supervision, Validation. **Keqin Li:** Supervision, Validation. **Jichun Li:** Writing - review & editing. **Lin Xiao:** Conceptualization, Methodology, Supervision, Investigation, Writing - review & editing.

Declaration of Competing Interest

The authors declare that they have no known competing financial interests or personal relationships that could have appeared to influence the work reported in this paper.

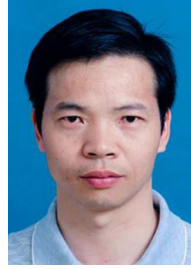
Acknowledgments

This work was supported by the National Key Research and Development Program of China (Grant No. 2016YFB0201800); the National Natural Science Foundation of China under grants 61866013, 61503152, 61976089, 61473259, and 61563017; the Natural Science Foundation of Hunan Province of China under grants 2019JJ50478, 18A289, JGY201926, 2016JJ2101, 2018TP1018, and 2018RS3065.

References

- [1] I. Mutlu, F. Schrödel, N. Bajcinca, D. Abel, M.T. Söylemez, Lyapunov equation based stability mapping approach: A MIMO case study, *IFAC-PapersOnLine* 49 (9) (2016) 130–135.
- [2] P. Benner, Solving large-scale control problems, *IEEE Control Syst. Mag.* 24 (1) (2004) 44–59.
- [3] Y. Qian, W. Pang, An implicit sequential algorithm for solving coupled Lyapunov equations of continuous-time Markovian jump systems, *Automatica* 60 (2015) 245–250.
- [4] B. Zhou, G. Duan, Z. Lin, A parametric periodic Lyapunov equation with application in semi-global stabilization of discrete-time periodic systems subject to actuator saturation, *Automatica* 47 (2) (2011) 316–325.
- [5] L. Xiao, B. Liao, S. Li, Z. Zhang, L. Ding, L. Jin, Design and analysis of FTZNN applied to the real-time solution of a nonstationary Lyapunov equation and tracking control of a wheeled mobile manipulator, *IEEE Trans. Ind. Inform.* 14 (1) (2018) 98–105.
- [6] Z. Li, B. Zhou, J. Lam, Y. Wang, Positive operator based iterative algorithms for solving Lyapunov equations for Itô stochastic systems with Markovian jumps, *Appl. Math. Comput.* 217 (21) (2011) 8179–8195.
- [7] F. Ding, H. Zhang, Gradient-based iterative algorithm for a class of the coupled matrix equations related to control systems, *IET Control Theory Appl.* 8 (15) (2014) 1588–1595.
- [8] Y. Lin, V. Simoncini, Minimal residual methods for large scale Lyapunov equations, *Appl. Numer. Math.* 72 (2013) 52–71.
- [9] L. Jin, S. Li, B. Hu, RNN models for dynamic matrix inversion: A control-theoretical perspective, *IEEE Trans. Ind. Inform.* 14 (1) (2017) 189–199.
- [10] Y. Zhang, Y. Yang, G. Ruan, Performance analysis of gradient neural network exploited for online time-varying quadratic minimization and equality-constrained quadratic programming, *Neurocomputing* 74 (10) (2011) 1710–1719.
- [11] D. Guo, C. Yi, Y. Zhang, Zhang neural network versus gradient-based neural network for time-varying linear matrix equation solving, *Neurocomputing* 74 (17) (2011) 3708–3712.
- [12] P. Stanimirović, M. Petković, Gradient neural dynamics for solving matrix equations and their applications, *Neurocomputing* 306 (2018) 200–212.
- [13] C. Yang, G. Peng, L. Cheng, J. Na, Z. Li, Force sensorless admittance control for teleoperation of uncertain robot manipulator using neural networks, *IEEE Trans. Syst. Man Cybern. Syst.*
- [14] Y. Zhang, K. Chen, X. Li, C. Yi, H. Zhu, Simulink modeling and comparison of Zhang neural networks and gradient neural networks for time-varying Lyapunov equation solving, in: 2008 Fourth International Conference on Natural Computation, vol. 3, IEEE, 2008, pp. 521–525.
- [15] Y. Zhang, K. Chen, H. Tan, Performance analysis of gradient neural network exploited for online time-varying matrix inversion, *IEEE Trans. Automat. Control* 54 (8) (2009) 1940–1945.
- [16] L. Xie, Y. Liu, H. Yang, Gradient based and least squares based iterative algorithms for matrix equations $AXB + CX^T D = F$, *Appl. Math. Comput.* 217 (5) (2010) 2191–2199.
- [17] L. Xiao, B. Liao, S. Li, K. Chen, Nonlinear recurrent neural networks for finite-time solution of general time-varying linear matrix equations, *Neural Netw.* 98 (2018) 102–113.
- [18] L. Xiao, Y. Zhang, Solving time-varying inverse kinematics problem of wheeled mobile manipulators using Zhang neural network with exponential convergence, *Nonlinear Dyn.* 76 (2) (2014) 1543–1559.
- [19] L. Xiao, A finite-time recurrent neural network for solving online time-varying Sylvester matrix equation based on a new evolution formula, *Nonlinear Dyn.* 90 (3) (2017) 1581–1591.
- [20] Y. Zhang, B. Qiu, B. Liao, Z. Yang, Control of pendulum tracking (including swinging up) of IPC system using zeroing-gradient method, *Nonlinear Dyn.* 89 (1) (2017) 1–25.
- [21] Z. Zhang, L. Zheng, J. Weng, Y. Mao, W. Lu, L. Xiao, A new varying-parameter recurrent neural-network for online solution of time-varying Sylvester equation, *IEEE Trans. Cybern.* 48 (11) (2018) 3135–3148.
- [22] Y. Xue, T. Tang, A. Liu, Large-scale feedforward neural network optimization by a self-adaptive strategy and parameter based particle swarm optimization, *IEEE Access* 7 (2019) 52473–52483.
- [23] Y. Xue, B. Xue, M. Zhang, Self-adaptive particle swarm optimization for large-scale feature selection in classification, *ACM Trans. Knowl. Discov. Data* 13 (5) (2019) 1–27.

- [24] Y. Xue, T. Tang, W. Peng, A. Liu, Self-adaptive parameter and strategy based particle swarm optimization for large-scale feature selection problems with multiple classifiers, *Appl. Soft Comput.* 88 (2020) 106031.
- [25] L. Xiao, A finite-time convergent neural dynamics for online solution of time-varying linear complex matrix equation, *Neurocomputing* 167 (2015) 254–259.
- [26] L. Jin, Y. Zhang, S. Li, Integration-enhanced Zhang neural network for real-time-varying matrix inversion in the presence of various kinds of noises, *IEEE Trans. Neural Netw. Learn. Syst.* 27 (12) (2015) 2615–2627.
- [27] L. Jin, Y. Zhang, S. Li, Y. Zhang, Noise-tolerant ZNN models for solving time-varying zero-finding problems: A control-theoretic approach, *IEEE Trans. Automat. Control* 62 (2) (2016) 992–997.
- [28] L. Jin, Y. Zhang, S. Li, Y. Zhang, Modified ZNN for time-varying quadratic programming with inherent tolerance to noises and its application to kinematic redundancy resolution of robot manipulators, *IEEE Trans. Ind. Electron.* 63 (11) (2016) 6978–6988.
- [29] L. Xiao, K. Li, M. Duan, Computing time-varying quadratic optimization with finite-time convergence and noise tolerance: A unified framework for Zeroing neural network, *IEEE Trans. Neural Netw. Learn. Syst.* 99 (1) (2019) 1–10.
- [30] C. Yi, Y. Chen, X. Lan, Comparison on neural solvers for the Lyapunov matrix equation with stationary & nonstationary coefficients, *Appl. Math. Model.* 37 (4) (2013) 2495–2502.
- [31] Y. Zhang, C. Yi, W. Ma, Simulation and verification of Zhang neural network for online time-varying matrix inversion, *Simul. Model. Pract. Theory* 17 (10) (2009) 1603–1617.
- [32] Q. Xiang, B. Liao, L. Xiao, L. Jin, A noise-tolerant Z-type neural network for time-dependent pseudoinverse matrices, *Optik* 165 (2018) 16–28.
- [33] S. Li, S. Chen, B. Liu, Accelerating a recurrent neural network to finite-time convergence for solving time-varying Sylvester equation by using a sign-bi-power activation function, *Neural Process. Lett.* 37 (2) (2013) 189–205.
- [34] L. Xiao, Z. Zhang, S. Li, Solving time-varying system of nonlinear equations by finite-time recurrent neural networks with application to motion tracking of robot manipulators, *IEEE Trans. Syst. Man Cybern. Syst.* 99 (1) (2019) 1–11.
- [35] A. Lamperski, A. Ames, Lyapunov theory for Zeno stability, *IEEE Trans. Automat. Control* 58 (1) (2012) 100–112.
- [36] Y. Zhang, C. Yi, D. Guo, J. Zheng, Comparison on Zhang neural dynamics and gradient-based neural dynamics for online solution of nonlinear time-varying equation, *Neural Comput. Appl.* 20 (1) (2011) 1–7.
- [37] D. Guo, Y. Zhang, Li-function activated ZNN with finite-time convergence applied to redundant-manipulator kinematic control via time-varying Jacobian matrix pseudoinversion, *Appl. Soft Comput.* 24 (2014) 158–168.
- [38] D. Chen, Y. Zhang, S. Li, Zeroing neural-dynamics approach and its robust and rapid solution for parallel robot manipulators against superposition of multiple disturbances, *Neurocomputing* 275 (2018) 845–858.
- [39] L. Jin, Y. Zhang, Discrete-time Zhang neural network of $O(\tau^3)$ pattern for time-varying matrix pseudoinversion with application to manipulator motion generation, *Neurocomputing* 142 (2014) 165–173.
- [40] L. Xiao, Y. Zhang, A new performance index for the repetitive motion of mobile manipulators, *IEEE Trans. Cybern.* 44 (2) (2014) 280–292.



Lin Xiao received the Ph.D. degree in Communication and Information Systems from Sun Yat-sen University, Guangzhou, China, in 2014. He is currently a Professor with the College of Information Science and Engineering, Hunan Normal University, Changsha, China. He has authored over 100 papers in international conferences and journals, such as the IEEE-TNNLS, the IEEE-TCYB, the IEEE-TII and the IEEE-TSMCA. His main research interests include neural networks, robotics, and intelligent information processing.



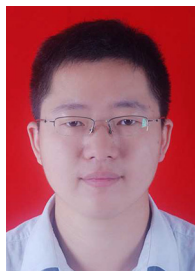
Kenli Li received the Ph.D. degree in computer science from the Huazhong University of Science and Technology, Wuhan, China, in 2003. He was a Visiting Scholar with the University of Illinois at Urbana-Champaign, Champaign, IL, USA, from 2004 to 2005. He is currently a Full Professor of Computer Science and Technology with Hunan University, Changsha, China, and also the Deputy Director of the National Supercomputing Center, Changsha. His current research interests include parallel computing, cloud computing, big data computing, and neural computing.



Jichun Li received his Ph.D. degree in mechanical engineering from King's College London, University of London, U.K. in 2013. He is currently a Lecturer with the School of Computer Science and Electronic Engineering, University of Essex, U.K. His main research interests include neural networks, robotics, intelligent transportation and communication, control, IoT and AI solutions for bespoke automated systems for chemical, medical, energy, agri-food and biosciences industries. He is a member of the IEEE, IET, and IMeChE.



Keqin Li is a SUNY Distinguished Professor of computer science with the State University of New York. He is also a Distinguished Professor at Hunan University, China. His current research interests include cloud computing, fog computing and mobile edge computing, energy-efficient computing and communication, embedded systems and cyberphysical systems, heterogeneous computing systems, big data computing, high-performance computing, CPU-GPU hybrid and cooperative computing, computer architectures and systems, computer networking, machine learning, intelligent and soft computing.



Zeshan Hu received the B.S. degree in Computer Science and Technology from Fuzhou University, Fuzhou, China, in 2018. He is currently a postgraduate with the College of Computer Science and Electronic Engineering, Hunan University, Changsha, China. His main research interests include neural networks, and robotics.